2-5-2018

Monte Carlo Simulations of Three-dimensional Electromagnetic Gaussian Schell-model Sources

Milo W. Hyde IV
Air Force Institute of Technology

Santasri Bose-Pillai
Air Force Institute of Technology

Olga Korotkova
University of Miami

Recommended Citation

Hyde IV, M. W., Bose-Pillai, S. R., & Korotkova, O. (2018). Monte carlo simulations of three-dimensional electromagnetic Gaussian Schell-model sources. Optics Express, 26(3), 2303–2313. https://doi.org/10.1364/OE.26.002303

Research Article | Vol. 26, No. 3 | 5 Feb 2018 | OPTICS EXPRESS 2303
Optics EXPRESS

Monte Carlo simulations of three-dimensional electromagnetic Gaussian Schell-model sources

Milo W. Hyde IV,[1,*] Santasri R. Bose-Pillai,[2,3] and Olga Korotkova[4,5]

[1] *Air Force Institute of Technology, Department of Electrical and Computer Engineering, 2950 Hobson Way, Dayton, OH 45433, USA*
[2] *Air Force Institute of Technology, Department of Engineering Physics, 2950 Hobson Way, Dayton, OH 45433, USA*
[3] *Srisys Inc., 7908 Cincinnati Dayton Road, West Chester Township, OH 45069, USA*
[4] *University of Miami, Department of Physics, 1320 Campo Sano Avenue, Coral Gables, FL 33146, USA*
[5] *Samara National Research University, Samara, 443086, Russia*
[*] *milo.hyde@us.af.mil*

Abstract: This article presents a method to simulate a three-dimensional (3D) electromagnetic Gaussian-Schell model (EGSM) source with desired characteristics. Using the complex screen method, originally developed for the synthesis of two-dimensional stochastic electromagnetic fields, a set of equations is derived which relate the desired 3D source characteristics to those of the statistics of the random complex screen. From these equations and the 3D EGSM source realizability conditions, a single criterion is derived, which when satisfied guarantees both the realizability and simulatability of the desired 3D EGSM source. Lastly, a 3D EGSM source, with specified properties, is simulated; the Monte Carlo simulation results are compared to the theoretical expressions to validate the method.

OCIS codes: (000.5490) Probability theory, stochastic processes, and statistics; (030.0030) Coherence and statistical optics; (030.1640) Coherence; (030.6600) Statistical optics.

References and links

1. L. Mandel and E. Wolf, *Optical Coherence and Quantum Optics* (Cambridge University, 1995).
2. E. Wolf, *Introduction to the Theory of Coherence and Polarization of Light* (Cambridge University, 2007).
3. O. Korotkova, *Random Light Beams: Theory and Applications* (CRC, 2014).
4. G. Gbur and T. Visser, "The structure of partially coherent fields," Prog. Opt. **55**, 285–341 (2010).
5. Y. Cai, Y. Chen, J. Yu, X. Liu, and L. Liu, "Generation of partially coherent beams," Prog. Opt. **62**, 157–223 (2017).
6. A. T. Friberg and T. Setälä, "Electromagnetic theory of optical coherence," J. Opt. Soc. Am. A **33**, 2431–2442 (2016).
7. G. Gbur, "Partially coherent beam propagation in atmospheric turbulence," J. Opt. Soc. Am. A **31**, 2038–2045 (2014).
8. Y. Cai, Y. Chen, and F. Wang, "Generation and propagation of partially coherent beams with nonconventional correlation functions: a review," J. Opt. Soc. Am. A **31**, 2083–2096 (2014).
9. Y. Chen, F. Wang, L. Liu, C. Zhao, Y. Cai, and O. Korotkova, "Generation and propagation of a partially coherent vector beam with special correlation functions," Phys. Rev. A **89**, 013801 (2014).
10. G. Piquero, F. Gori, P. Romanini, M. Santarsiero, R. Borghi, and A. Mondello, "Synthesis of partially polarized Gaussian Schell-model sources," Opt. Commun. **208**, 9–16 (2002).
11. T. Shirai, O. Korotkova, and E. Wolf, "A method of generating electromagnetic Gaussian Schell-model beams," J. Opt. A: Pure Appl. Opt. **7**, 232–237 (2005).
12. S. Avramov-Zamurovic, C. Nelson, R. Malek-Madani, and O. Korotkova, "Polarization-induced reduction in scintillation of optical beams propagating in simulated turbulent atmospheric channels," Waves Random Complex Media **24**, 452–462 (2014).
13. I. Iliopoulos, M. Casaletti, R. Sauleau, P. Pouliguen, P. Potier, and M. Ettorre, "3-D shaping of a focused aperture in the near field," IEEE Trans. Antennas Propag. **64**, 5262–5271 (2016).
14. J. A. Rodrigo, T. Alieva, E. Abramochkin, and I. Castro, "Shaping of light beams along curves in three dimensions," Opt. Express **21**, 20544–20555 (2013).
15. J. Hao, Z. Yu, H. Chen, Z. Chen, H.-T. Wang, and J. Ding, "Light field shaping by tailoring both phase and polarization," Appl. Opt. **53**, 785–791 (2014).
16. C. Chang, Y. Gao, J. Xia, S. Nie, and J. Ding, "Shaping of optical vector beams in three dimensions," Opt. Lett. **42**, 3884–3887 (2017).

#308701 https://doi.org/10.1364/OE.26.002303
Journal © 2018 Received 6 Oct 2017; accepted 4 Jan 2018; published 23 Jan 2018

Optics EXPRESS

17. J. Tervo, T. Setälä, and A. T. Friberg, "Degree of coherence for electromagnetic fields," Opt. Express **11**, 1137–1143 (2003).
18. O. Korotkova and E. Wolf, "Spectral degree of coherence of a random three-dimensional electromagnetic field," J. Opt. Soc. Am. A **21**, 2382–2385 (2004).
19. Z. Mei, "Generalized Stokes parameters of three-dimensional stochastic electromagnetic beams," Opt. Express **18**, 22826–22832 (2010).
20. T. Setälä, A. Shevchenko, M. Kaivola, and A. T. Friberg, "Degree of polarization for optical near fields," Phys. Rev. E **66**, 016615 (2002).
21. J. Ellis, A. Dogariu, S. Ponomarenko, and E. Wolf, "Degree of polarization of statistically stationary electromagnetic fields," Opt. Commun. **248**, 333–337 (2005).
22. O. Korotkova, L. Ahad, and T. Setälä, "Three-dimensional electromagnetic Gaussian Schell-model sources," Opt. Lett. **42**, 1792–1795 (2017).
23. D. Voelz, X. Xiao, and O. Korotkova, "Numerical modeling of Schell-model beams with arbitrary far-field patterns," Opt. Lett. **40**, 352–355 (2015).
24. S. Basu, M. W. Hyde, X. Xiao, D. G. Voelz, and O. Korotkova, "Computational approaches for generating electromagnetic Gaussian Schell-model sources," Opt. Express **22**, 31691–31707 (2014).
25. X. Xiao, D. G. Voelz, S. R. Bose-Pillai, and M. W. Hyde, "Modeling random screens for predefined electromagnetic Gaussian-Schell model sources," Opt. Express **25**, 3656–3665 (2017).
26. X. Xiao and D. Voelz, "Wave optics simulation approach for partial spatially coherent beams," Opt. Express **14**, 6986–6992 (2006).
27. M. W. Hyde IV, S. Basu, D. G. Voelz, and X. Xiao, "Generating partially coherent Schell-model sources using a modified phase screen approach," Opt. Eng. **54**, 120501 (2015).
28. M. W. Hyde, S. Bose-Pillai, D. G. Voelz, and X. Xiao, "Generation of vector partially coherent optical sources using phase-only spatial light modulators," Phys. Rev. Applied **6**, 064030 (2016).
29. C. A. Mack, "Generating random rough edges, surfaces, and volumes," Appl. Opt. **52**, 1472–1480 (2013).
30. H. T. Yura and S. G. Hanson, "Digital simulation of an arbitrary stationary stochastic process by spectral representation," J. Opt. Soc. Am. A **28**, 675–685 (2011).

1. Introduction

The behavior of two-dimensional (2D) stochastic electromagnetic (EM) fields has and continues to be an important and popular topic of optics research [1–6]. This area of study is quite mature and optical systems that exploit coherence and polarization to beam shape, mitigate atmospheric scintillation, or reduce speckle are being developed [7–12].

For certain scenarios, e.g., near-field beam shaping [13–16], observing in the near zone of a scatterer, or observing in the vicinity of a caustic, a full, three-dimensional (3D) vector treatment of the field is required. The study of light's behavior under these and other similar conditions motivates research involving 3D stochastic EM fields. Much of the published work on this subject involves defining physically significant statistics of 3D random EM fields, most notably, the degree of coherence [17, 18], Stokes parameters [19], and the degree of polarization [20, 21]. To date, little work has been performed developing 3D random field models (counterparts to the ubiquitous Schell-model sources in 1D and 2D) or in synthesizing 3D random field instances.

Here, a method to simulate a 3D electromagnetic Gaussian Schell-model (EGSM) source with desired shape and coherence properties is presented. The 3D EGSM source was recently introduced in Ref. [22]. There, the authors derived a set of conditions that all 3D EGSM sources must satisfy in order to be physically realizable sources.

Using the complex screen method (originally developed for the synthesis of 2D random fields) [23–25], equations relating the desired 3D EGSM source parameters (source widths, spatial correlation radii, et cetera) to the random complex screen parameters are derived. Then, using these equations and the realizability conditions developed in Ref. [22], a single criterion is found, which when satisfied guarantees that the desired 3D EGSM source is both realizable and simulatable. Lastly, a 3D EGSM source, with specified properties, is simulated using the 3D complex screen method. The simulated results are compared to the analytical expressions to validate the analysis.

It should be noted that no device or method for physically realizing a designer 3D EGSM source currently exists. Nevertheless, the work presented here provides a recipe for generating

Optics EXPRESS

such a source should the technology become available. This work can be put to immediate use in wave optics simulations of scenarios similar to those mentioned above.

2. Theory

The cross-spectral density matrix elements of a 3D EGSM source take the form

$$W_{ij}(\boldsymbol{r}_1, \boldsymbol{r}_2) = A_i A_j B_{ij} \exp\left(-\frac{r_1^2}{4\sigma_i^2}\right) \exp\left(-\frac{r_2^2}{4\sigma_j^2}\right) \exp\left(-\frac{|\boldsymbol{r}_1 - \boldsymbol{r}_2|^2}{2\delta_{ij}^2}\right), \tag{1}$$

where $i, j = x, y, z$, A_i is the amplitude of the i^{th} field component, B_{ij} is the complex cross-correlation coefficient between the i^{th} and j^{th} components, σ_i is the spectral density width of the i^{th} component, δ_{ij} is the width of the cross-correlation function between the i^{th} and j^{th} components, and $\boldsymbol{r} = \hat{\boldsymbol{x}}x + \hat{\boldsymbol{y}}y + \hat{\boldsymbol{z}}z$ [22]. For the 3D EGSM source to be physically realizable, the δ_{ij} and B_{ij} must satisfy [22]

$$\delta_{ij} = \delta_{ji} \tag{2}$$

$$B_{ij} = B_{ji}^* \tag{3}$$

$$\delta_{ii}^2 + \delta_{jj}^2 \leq 2\delta_{ij}^2 \tag{4}$$

$$\begin{aligned} &|B_{xy}|^2 \left(\frac{\delta_{xy}^2}{\delta_{xx}\delta_{yy}}\right)^3 + |B_{xz}|^2 \left(\frac{\delta_{xz}^2}{\delta_{xx}\delta_{zz}}\right)^3 + |B_{yz}|^2 \left(\frac{\delta_{yz}^2}{\delta_{yy}\delta_{zz}}\right)^3 \\ &\leq 1 - 2|B_{xy}||B_{xz}||B_{yz}| \left(\frac{\delta_{xy}\delta_{xz}\delta_{yz}}{\delta_{xx}\delta_{yy}\delta_{zz}}\right)^3 \end{aligned}. \tag{5}$$

In addition, $B_{ii} = 1$ and $|B_{ij}| \leq 1$ when $i \neq j$.

Generating 3D EGSM sources can be accomplished by using extensions of the techniques discussed in Refs. [24–26]. Since it forms the basis of the modified phase screen technique [27,28], the complex transmittance screen approach (in this context, more accurately termed the complex volume approach) is presented here. The traditional Gaussian phase screen [24–26] details can be derived in a similar manner; for completeness, the phase screen expressions are provided in Appendix A.

Let an instance of the i^{th} component of a 3D EGSM source be

$$E_i(\boldsymbol{r}) = C_i \exp\left(-\frac{r^2}{4\sigma_i^2}\right) T_i(\boldsymbol{r}), \tag{6}$$

where C_i is the complex amplitude and T_i is the random complex transmittance screen. Taking the vector autocorrelation of Eq. (6) produces

$$\langle E_i(\boldsymbol{r}_1) E_j^*(\boldsymbol{r}_1)\rangle = C_i C_j^* \exp\left(-\frac{r_1^2}{4\sigma_i^2}\right) \exp\left(-\frac{r_2^2}{4\sigma_j^2}\right) \langle T_i(\boldsymbol{r}_1) T_j^*(\boldsymbol{r}_2)\rangle. \tag{7}$$

Comparing Eqs. (7) and (1) reveals the following:

$$\begin{aligned} |C_i| &= A_i \\ \arg\left(C_i C_j^*\right) &= \arg\left(B_{ij}\right) \\ \langle T_i(\boldsymbol{r}_1) T_i^*(\boldsymbol{r}_2)\rangle &= \exp\left(-\frac{|\boldsymbol{r}_1 - \boldsymbol{r}_2|^2}{2\delta_{ii}^2}\right) \\ \langle T_i(\boldsymbol{r}_1) T_j^*(\boldsymbol{r}_2)\rangle &= |B_{ij}| \exp\left(-\frac{|\boldsymbol{r}_1 - \boldsymbol{r}_2|^2}{2\delta_{ij}^2}\right) \end{aligned}. \tag{8}$$

One is free to choose the amplitudes A_i and the spectral density widths σ_i of the 3D EGSM source. The phase angles $\arg\left(B_{ij}\right)$ are solutions to

$$\begin{pmatrix} 1 & -1 & 0 \\ 1 & 0 & -1 \\ 0 & 1 & -1 \end{pmatrix} \begin{pmatrix} \alpha_x \\ \alpha_y \\ \alpha_z \end{pmatrix} = \begin{pmatrix} \theta_{xy} \\ \theta_{xz} \\ \theta_{yz} \end{pmatrix}, \tag{9}$$

where $\alpha_i = \arg\left(C_i\right)$ and $\theta_{ij} = \arg\left(B_{ij}\right)$. Solving the above system of equations reveals that $\theta_{xy} + \theta_{yz} = \theta_{xz}$; thus, two of the three phase angles can be chosen freely, the last is determined by the other two. This stands in contrast to the 2D case where one is free to choose the phase angle [24].

Lastly, the $\left|B_{ij}\right|$ and δ_{ij} are coupled and even if realizable [i.e., the desired values satisfy Eqs. (2)–(5)], the source they describe may not be *simulatable* using the complex screen approach. The question of whether a desired 3D EGSM source is simulatable is addressed in the next section.

2.1. T_i generation

A complex screen T_i can be generated using the Monte Carlo spectral method (MCSM) [23, 24, 29, 30]. Using the MCSM (not reviewed here), a realization of T_i takes the form

$$T_i\left[i,j,k\right] = \sum_{l,m,n} r_i\left[l,m,n\right] \sqrt{\frac{\Phi_{ii}\left[l,m,n\right]}{2L_xL_yL_z}} \exp\left(\mathrm{j}\frac{2\pi}{L_x}li\right) \exp\left(\mathrm{j}\frac{2\pi}{L_y}mj\right) \exp\left(\mathrm{j}\frac{2\pi}{L_z}nk\right), \tag{10}$$

where i, j, k are discrete spatial indices, l, m, n are discrete spatial frequency indices, r_i is a 3D matrix of zero-mean, unit-variance circular complex Gaussian random numbers, L_x, L_y, L_z are the physical sizes of the grid in the x, y, and z directions, respectively, and Φ_{ii} is the spatial power spectrum of the screen:

$$\begin{aligned} \Phi_{ii}\left(\boldsymbol{f}\right) &= \iiint_{-\infty}^{\infty} \exp\left(-\frac{r^2}{2\delta_{ii}^2}\right) \exp\left(-\mathrm{j}2\pi\boldsymbol{f}\cdot\boldsymbol{r}\right) \mathrm{d}^3r \\ &= \left(2\pi\delta_{ii}^2\right)^{3/2} \exp\left(-2\pi^2\delta_{ii}^2f^2\right) \end{aligned}. \tag{11}$$

Note that Eq. (10) is in the form of a discrete inverse Fourier transform; thus, T_i can be generated quickly using the fast Fourier transform algorithm.

Generating T_i using Eq. (10) will produce a screen with the desired δ_{ii} and, via Eq. (6), a 3D EGSM source with the desired W_{ii}. To produce a 3D EGSM source with the desired W_{ij} requires examination of the cross-correlation of the T_i and T_j screens, namely,

$$\begin{aligned} \left\langle T_i\left[i_1,j_1,k_1\right] T_j^*\left[i_2,j_2,k_2\right]\right\rangle &= \sum_{l_1,m_1,n_1} \sum_{l_2,m_2,n_2} \left\langle r_i\left[l_1,m_1,n_1\right] r_j^*\left[l_2,m_2,n_2\right]\right\rangle \\ &\times \frac{\sqrt{\Phi_{ii}\left[l_1,m_1,n_1\right]\Phi_{jj}\left[l_2,m_2,n_2\right]}}{2L_xL_yL_z} \exp\left[\mathrm{j}\frac{2\pi}{L_x}\left(l_1i_1 - l_2i_2\right)\right] \exp\left[\mathrm{j}\frac{2\pi}{L_y}\left(m_1j_1 - m_2j_2\right)\right] \\ &\times \exp\left[\mathrm{j}\frac{2\pi}{L_z}\left(n_1k_1 - n_2k_2\right)\right] \end{aligned}. \tag{12}$$

The moment in Eq. (12) is $2\Gamma_{ij}\delta\left[l_1 - l_2\right]\delta\left[m_1 - m_2\right]\delta\left[n_1 - n_2\right]$, where δ is the discrete Dirac delta function and $0 \le \Gamma_{ij} \le 1$ is the correlation coefficient between the 3D matrices of Gaussian random numbers r_i and r_j. Substituting in the expressions for the spatial power spectra [recall

Optics EXPRESS

Eq. (11)] and simplifying yields

$$\begin{aligned}\langle T_i[i_1,j_1,k_1]\,T_j^*[i_2,j_2,k_2]\rangle &= \sum_{l,m,n}\left\{\Gamma_{ij}\left(2\pi\delta_{ii}\delta_{jj}\right)^{3/2}\exp\left[-\pi^2\left(\delta_{ii}^2+\delta_{jj}^2\right)\left(l^2+m^2+n^2\right)\right]\right\}\\ &\times\exp\left[\mathrm{j}\frac{2\pi}{L_x}l\left(i_1-i_2\right)\right]\exp\left[\mathrm{j}\frac{2\pi}{L_y}m\left(j_1-j_2\right)\right]\exp\left[\mathrm{j}\frac{2\pi}{L_z}n\left(k_1-k_2\right)\right]\end{aligned}. \tag{13}$$

The expression in the braces must equal the spatial cross-power spectrum,

$$\begin{aligned}\Phi_{ij}(\boldsymbol{f}) &= \iiint_{-\infty}^{\infty}\left|B_{ij}\right|\exp\left(-\frac{r^2}{2\delta_{ij}^2}\right)\exp\left(-\mathrm{j}2\pi\boldsymbol{f}\cdot\boldsymbol{r}\right)\mathrm{d}^3r\\ &= \left|B_{ij}\right|\left(2\pi\delta_{ij}^2\right)^{3/2}\exp\left(-2\pi^2\delta_{ij}^2f^2\right)\end{aligned}, \tag{14}$$

to produce the desired 3D EGSM source. Comparing the braced expression in Eq. (13) with Eq. (14), it is clear that

$$\begin{aligned}\delta_{ij} &= \sqrt{\frac{\delta_{ii}^2+\delta_{jj}^2}{2}}\\ \left|B_{ij}\right| &= \Gamma_{ij}\left(\frac{\delta_{ii}\delta_{jj}}{\delta_{ij}^2}\right)^{3/2} = \Gamma_{ij}\left(\frac{2\delta_{ii}\delta_{jj}}{\delta_{ii}^2+\delta_{jj}^2}\right)^{3/2}.\end{aligned} \tag{15}$$

Thus, the relationships between the 3D EGSM source and complex screen parameters are

$$A_i = |C_i| \tag{16}$$

$$\arg\left(B_{ij}\right) = \arg\left(C_iC_j^*\right) \tag{17}$$

$$\delta_{ij} = \sqrt{\frac{\delta_{ii}^2+\delta_{jj}^2}{2}} \tag{18}$$

$$\left|B_{ij}\right| = \Gamma_{ij}\frac{2\delta_{ii}\delta_{jj}}{\delta_{ii}^2+\delta_{jj}^2}\sqrt{\frac{2\delta_{ii}\delta_{jj}}{\delta_{ii}^2+\delta_{jj}^2}}. \tag{19}$$

These expressions are very similar to the 2D EGSM source complex screen relations given in Ref. [24]—the only difference being the square root term in Eq. (19). Note that the values of δ_{ij} are set by the values of the corresponding "self" correlation radii exactly the same as in the 2D case [see Eq. (18)]. Equation (18) always satisfies the δ_{ij} realizability condition in Eq. (4).

Examining Eq. (19), it initially appears, like in the 2D case, that one is generally free to choose the values of $\left|B_{ij}\right|$ granted $0 \le \Gamma_{ij} \le 1$. This, however, is not the case. Returning to the $\left|B_{ij}\right|$ realizability condition given in Eq. (5) and substituting in Eqs. (18) and (19) yields

$$\Gamma_{xy}^2+\Gamma_{xz}^2+\Gamma_{yz}^2+2\Gamma_{xy}\Gamma_{xz}\Gamma_{yz}-1 \le 0. \tag{20}$$

A 3D plot of this simulatability condition is shown in Fig. 1. Figure 1(a) shows a view of the volume's surface with the interior removed and (b) shows a view of the surface from a different angle. The volume intersects each primary plane in a quarter circle. Any Γ_{ij} combination that results in a point within the volume (underneath the surface in Fig. 1) is both a realizable and simulatable 3D EGSM source. If $\Gamma_{xz} = \Gamma_{yz} = 0$, implying that $|B_{xz}| = \left|B_{yz}\right| = 0$ (physically reducing a 3D EGSM source to a 2D one, assuming that $W_{zz} = 0$), then Eq. (20) reduces to $\Gamma_{xy} \le 1$ which is always true. Thus, satisfying Eq. (20) guarantees realizability and simulatability of that particular 3D EGSM source as well as all 2D EGSM sources which can be derived from it.

Optics EXPRESS

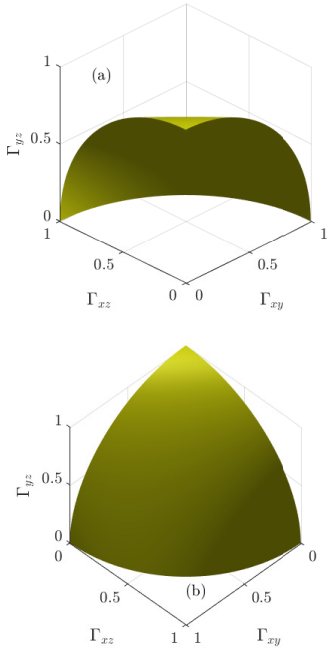

Fig. 1. Complex screen 3D EGSM source simulatability condition given in Eq. (20)—(a) view of volume's surface with interior removed and (b) different view of surface.

2.2. *Summary of 3D EGSM source simulation process*

Before proceeding to the simulation results, a step-by-step description of the complex screen 3D EGSM source simulation process is warranted:

1. Choose values for the free source parameters σ_i and A_i, which are related to the screen parameters $|C_i|$ via Eq. (16).

2. Choose values for the phase angles $\arg\left(B_{ij}\right) = \theta_{ij}$, which are related to $\arg\left(C_i C_j^*\right)$ via Eq. (17). Recall that $\theta_{xy} + \theta_{yz} - \theta_{xz} = 0$. The pseudoinverse of the matrix in Eq. (9) can be used to find simulatable phase angles which are closest (minimum Euclidean norm) to a set of three desired phase angles.

3. Choose values for the coupled source parameters δ_{ij} and $\left|B_{ij}\right|$. Recall that δ_{ij} is set by the values of δ_{ii} and δ_{jj} [see Eq. (18)].

4. Ensure source realizability [see Eqs. (2)–(5)] and simulatability [see Eq. (20)]. Steps 3 and 4 can be combined into a single step where the desired coupled parameters are inputs into a constrained nonlinear optimization routine that returns the screen parameters δ_{ii}, δ_{jj}, and Γ_{ij} which yield realizable and simulatable source parameters closest (by minimizing a user specified norm) to the desired parameters.

5. Generate 3 3D matrices of correlated, zero-mean, unit-variance circular complex Gaussian random numbers r_i. The covariance matrix is formed from the values of Γ_{ij} found in step 4.

6. Generate a T_i realization using Eq. (10).

7. Form 3D EGSM source instance E_i using Eq. (6).

Optics EXPRESS

3. Simulation

3.1. Simulation details

Table 1. 3D EGSM Source Parameters

A_x	1
A_y	1.5
A_z	2
σ_x	4 cm
σ_y	5 cm
σ_z	10 cm
δ_{xx}	2 cm
δ_{yy}	3 cm
δ_{zz}	5 cm
δ_{xy}	2.55 cm
δ_{xz}	3.81 cm
δ_{yz}	4.12 cm
B_{xy}	$0.222 \exp(\mathrm{j}\pi/2)$
B_{xz}	$0.286 \exp(\mathrm{j}\pi/3)$
B_{yz}	$0.539 \exp(-\mathrm{j}\pi/6)$

To validate the above analysis, a 3D EGSM source was simulated using the complex screen technique. The EGSM source parameters are listed in Table 1. The computational volume was discretized using 512 points per side with a sample spacing equal to 1.37 mm, making the total physical size of the grid 0.7 m × 0.7 m × 0.7 m. The component spectral densities S_i and spectral degrees of correlation μ_{ij},

$$S_i(\boldsymbol{r}) = W_{ii}(\boldsymbol{r},\boldsymbol{r}) = \langle |E_i(\boldsymbol{r})|^2 \rangle$$
$$\mu_{ij}(\boldsymbol{r}_1,\boldsymbol{r}_2) = \frac{W_{ij}(\boldsymbol{r}_1,\boldsymbol{r}_2)}{\sqrt{S_i(\boldsymbol{r}_1) S_j(\boldsymbol{r}_2)}}, \tag{21}$$

were computed from 500 complex screen field instances. The simulated S_i and μ_{ij} were then compared to the corresponding theoretical quantities to verify that the desired 3D EGSM source had been realized.

3.2. Results

3.2.1. Spectral densities S_i

Figures 2 and 3 show spectral density S results. To give the reader an understanding of what a complex screen 3D EGSM source looks like, Fig. 2 shows two views of the spectral density volume computed from a single realization of the 3D EGSM source whose parameters are given in Table 1. Figure 2(a) shows a view of the volume's surface, while Fig. 2(b) shows the x-y, x-z, and y-z planar slices through the volume.

Figure 3 shows the theoretical (solid traces) and simulated (circles) (a) x, (b) y, and (c) z spectral densities, respectively. The agreement between the simulated and theoretical results is excellent. These results verify that the complex screens, on average, are producing a 3D EGSM source with the desired shape. To verify that the resulting source has the desired coherence properties, the spectral degrees of correlation μ_{ij} must be examined.

3.2.2. Spectral degrees of correlation μ_{ij}

Figures 4 and 5 show spectral degree of correlation results. Figure 4 shows the theoretical (solid traces) and simulated (circles) (a) μ_{xx}, (b) μ_{yy}, and (c) μ_{zz} results, respectively; Fig. 5 shows the

Optics EXPRESS

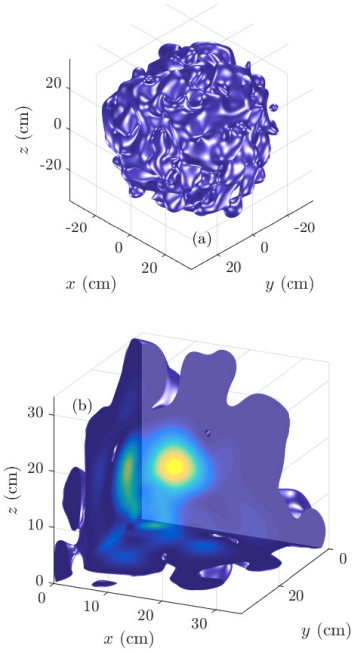

Fig. 2. Single realization spectral density volume of the complex screen 3D EGSM source whose parameters are given in Table 1—(a) surface view and (b) x-y, x-z, and y-z planar slices.

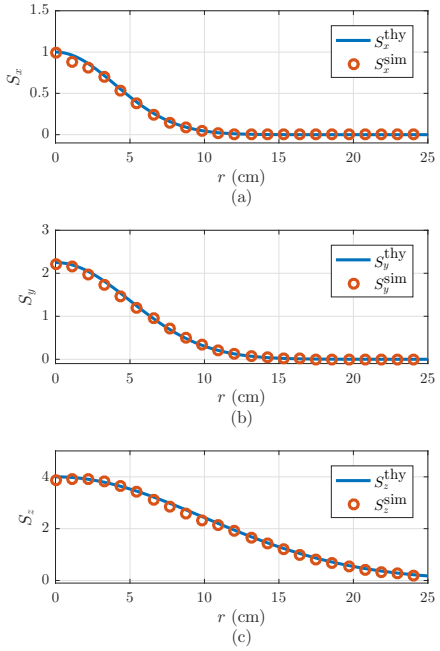

Fig. 3. Spectral densities theory (solid traces) versus simulation (circles) in the (a) x, (b) y, and (c) z directions.

Optics EXPRESS

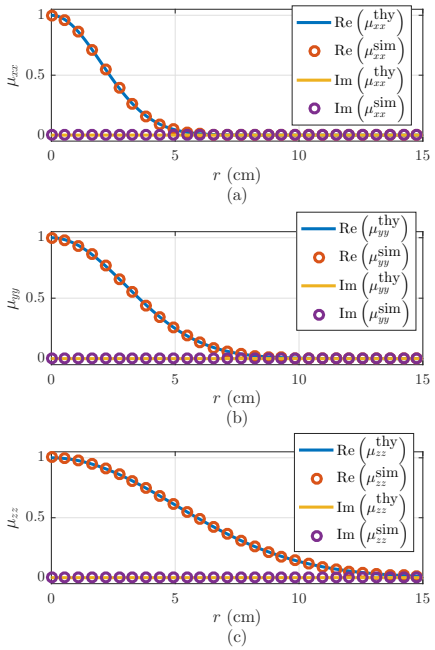

Fig. 4. Spectral degrees of correlation theory (solid traces) versus simulation (circles)—(a) real and imaginary parts of μ_{xx}, (b) real and imaginary parts of μ_{yy}, and (c) real and imaginary parts of μ_{zz}.

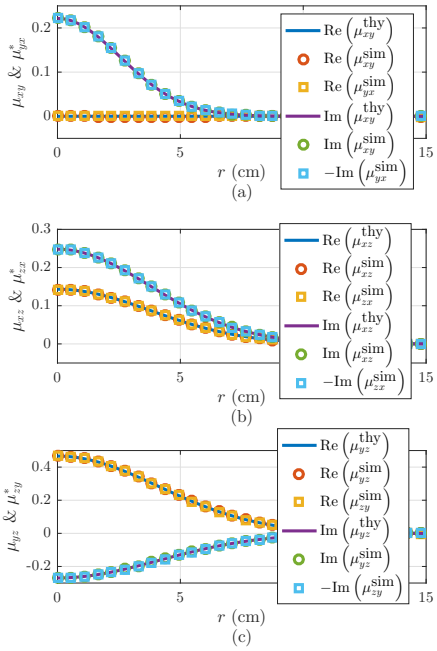

Fig. 5. Spectral degrees of correlation theory (solid traces) versus simulation (circles and squares)—(a) real and imaginary parts of μ_{xy} and μ_{yx}^{*}, (b) real and imaginary parts of μ_{xz} and μ_{zx}^{*}, and (c) real and imaginary parts of μ_{yz} and μ_{zy}^{*}.

Optics EXPRESS

theoretical (solid traces) and simulated (circles and squares) (a) μ_{xy} and μ^*_{yx}, (b) μ_{xz} and μ^*_{zx}, and (c) μ_{yz} and μ^*_{zy}, respectively. In Figs. 4 and 5, both the real and imaginary parts of μ_{ij} are plotted.

Again, the agreement between the simulated and theoretical results is excellent. These results combined with the spectral density results in Fig. 3 validate the complex screen simulation procedure developed in Section 2.

4. Conclusion

In this paper, the simulation of a 3D EGSM source using the complex screen technique was investigated. Relationships between the source parameters (A_i, B_{ij}, σ_i, and δ_{ij}) and the complex screen parameters were derived and discussed. Using these expressions and the recently published 3D EGSM source realizability conditions [22] yielded a new, single simulatability criterion. When satisfied, this condition guaranteed both realizability and simulatability of the desired 3D EGSM source using the complex screen method.

To validate the analysis, a 3D EGSM source was simulated using the complex screen technique. The simulated directional spectral densities and spectral degrees of correlation were compared to those of the true 3D EGSM source. The agreement between the simulated and theoretical results was excellent.

Although no device or method for physically realizing a desired 3D EGSM source yet exists, this paper provides the basic recipe for generating such a source if or when the technology becomes available. In the meantime, the technique and procedure for simulating 3D EGSM sources developed here will find use in optical simulations involving non-paraxial, partially coherent EM fields, e.g., in simulations where a random field is observed in the near zone of a scatterer or in the vicinity of a tight focus, or caustic.

A. Phase screen 3D EGSM Sources

An instance of the i^{th} component of a phase screen 3D EGSM source is

$$E_i(\boldsymbol{r}) = C_i \exp\left(-\frac{r^2}{4\sigma_i^2}\right) \exp\left[\mathrm{j}\phi_i(\boldsymbol{r})\right], \tag{22}$$

where ϕ_i is the random 3D phase screen. The relationships between the 3D EGSM source and phase screen parameters are

$$A_i = |C_i| \tag{23}$$

$$\arg\left(B_{ij}\right) = \arg\left(C_i C_j^*\right) \tag{24}$$

$$\delta_{ii} = \frac{\ell_{\phi_i\phi_i}}{\sqrt{2}\sigma_{\phi_i}} \tag{25}$$

$$\delta_{ij} = \frac{1}{\sqrt{2}} \frac{\ell^2_{\phi_i\phi_i} + \ell^2_{\phi_j\phi_j}}{\sqrt{4\Gamma_{\phi_i\phi_j}\sigma_{\phi_i}\sigma_{\phi_j}\ell_{\phi_i\phi_i}\ell_{\phi_j\phi_j}}} \left(\frac{\ell^2_{\phi_i\phi_i} + \ell^2_{\phi_j\phi_j}}{2\ell_{\phi_i\phi_i}\ell_{\phi_j\phi_j}}\right)^{1/4} \tag{26}$$

$$\left|B_{ij}\right| = \exp\left[-\frac{1}{2}\left(\sigma^2_{\phi_i} - \frac{4\Gamma_{\phi_i\phi_j}\sigma_{\phi_i}\sigma_{\phi_j}\ell_{\phi_i\phi_i}\ell_{\phi_j\phi_j}}{\ell^2_{\phi_i\phi_i} + \ell^2_{\phi_j\phi_j}} \sqrt{\frac{2\ell_{\phi_i\phi_i}\ell_{\phi_j\phi_j}}{\ell^2_{\phi_i\phi_i} + \ell^2_{\phi_j\phi_j}}} + \sigma^2_{\phi_j}\right)\right] \tag{27}$$

$$\sigma_{\phi_i}, \sigma_{\phi_j} \geq \pi, \tag{28}$$

where $0 \leq \Gamma_{\phi_i\phi_j} \leq 1$ is the correlation coefficient between the i^{th} and j^{th} component phase screens and $\sigma^2_{\phi_i}$ and $\ell_{\phi_i\phi_i}$ are the variance and spatial correlation radius of the i^{th} component phase screen, respectively.

Optics EXPRESS

Via the MCSM, a phase screen instance can be generated by using

$$\phi_i[i,j,k] = \mathrm{Re}\left\{\sum_{l,m,n} r_i[l,m,n]\sqrt{\frac{\Phi_{\phi_i\phi_i}[l,m,n]}{L_xL_yL_z}}\exp\left(\mathrm{j}\frac{2\pi}{L_x}li\right)\exp\left(\mathrm{j}\frac{2\pi}{L_y}mj\right)\exp\left(\mathrm{j}\frac{2\pi}{L_z}nk\right)\right\}, \tag{29}$$

where $\Phi_{\phi_i\phi_i}$ is the spatial power spectrum of the i^{th} component screen, namely,

$$\begin{aligned}\Phi_{\phi_i\phi_i}(\boldsymbol{f}) &= \iiint_{-\infty}^{\infty}\sigma_{\phi_i}^2\exp\left(-\frac{r^2}{\ell_{\phi_i\phi_i}^2}\right)\exp\left(-\mathrm{j}2\pi\boldsymbol{f}\cdot\boldsymbol{r}\right)\mathrm{d}^3r\\ &= \sigma_{\phi_i}^2\left(\pi\ell_{\phi_i\phi_i}^2\right)^{3/2}\exp\left(-\pi^2\ell_{\phi_i\phi_i}^2f^2\right)\end{aligned} \tag{30}$$

and r_i is a 3D matrix of zero-mean, unit-variance circular complex Gaussian random numbers.

The steps for generating a phase screen 3D EGSM source instance are generally the same as the complex screen steps listed above. Because of the complicated nonlinear equations relating the source parameters to the phase screen parameters [see Eqs. (25)–(28)], steps 3 and 4 of the source simulation process are much more difficult than in the complex screen case.

Funding

Air Force Office of Scientific Research (AFOSR) (FA9550-121-0449); Russian Federation Ministry of Education and Science.

Acknowledgments

The views expressed in this paper are those of the authors and do not reflect the official policy or position of the US Air Force, the Department of Defense, or the US government.